INDIAN JOURNAL OF SCIENCE AND TECHNOLOGY

ORIGINAL ARTICLE

OPEN ACCESS

Received: 28/12/2025

Accepted: 20/01/2026

Published: 30/01/2026

Citation: Ashokkumar G, Kannan R, Ravi A (2026) Modelling and Control of a PV System with INC-Based MPPT and Luo Converter for Motor Drive Applications. Indian Journal of Science and Technology 19(4): 232-244. https://doi.org/10.17485/IJST/v19i4.2039

* **Corresponding author**.

nveeramurgan@gmail.com

Funding: None

Competing Interests: None

Published By Indian Society for Education and Environment (iSee)

ISSN
Print: 0974-6846
Electronic: 0974-5645

Modelling and Control of a PV System with INC-Based MPPT and Luo Converter for Motor Drive Applications

G Ashokkumar[1]*, R Kannan[1], A Ravi[2]

1 Department of Electrical Engineering, FEAT, Annamalai University, Annamalainagar, Tamil Nadu, India
2 Department of Electrical and Electronics Engineering, A.V.C College of Engineering, Mayiladuthurai, Tamil Nadu, India

Abstract

Objectives: The objective of this study is to develop and evaluate a standalone photovoltaic (PV)–driven variable-speed induction motor system using an Incremental Conductance (INC)–based maximum power point tracking (MPPT) algorithm and a positive-output super-lift Luo (POSLL) DC–DC converter, and to quantitatively compare SPWM and SVPWM inverter control strategies under varying operating conditions. **Methods:** The proposed system is modeled in MATLAB/Simulink and comprises a PV array, INC-MPPT controller, POSLL DC–DC converter, and a three-phase voltage source inverter feeding a closed-loop induction motor drive. System performance is examined under irradiance variations from 1000 W/m^2 to 200 W/m^2, speed transients, and load disturbances. SPWM and SVPWM techniques are evaluated using identical test conditions. **Findings:** Simulation results show that the INC-MPPT maintains stable power extraction and regulates the DC-link voltage at approximately 250 V despite irradiance fluctuations. The POSLL converter provides high voltage gain with reduced ripple, ensuring continuous motor operation. Compared to SPWM, SVPWM reduces startup settling time from 0.364 s to 0.1232 s and improves steady-state efficiency from 95.84% to 98.46%. Under load disturbance, SVPWM maintains higher efficiency than SPWM, indicating improved dynamic stability and disturbance rejection. **Novelty:** This work presents a system-level integration and quantitative validation of an INC-MPPT-controlled POSLL converter combined with SVPWM-based inverter control for standalone PV-fed induction motor applications, demonstrating superior dynamic response and efficiency compared to conventional SPWM-based systems.

Keywords: Photovoltaic (PV) System; Incremental Conductance (INC) Algorithm; Maximum Power Point Tracking (MPPT); Positive Output Super-Lift Luo (POSLL) Converter; Voltage Source Inverter (VSI); Induction Motor Drive

1 Introduction

The global shift towards sustainable energy solutions has intensified the adoption of solar power systems, driven by their environmental and economic benefits. Solar energy is abundant, environmentally friendly, and economical in nature. This is particularly useful in regions without a constant electricity supply [1]. Solar panels achieve peak efficiency at a specific operational point, referred to as the Maximum Power Point (MPP), where the energy output is maximized. Maximum Power Point Tracking (MPPT) techniques are used to maximize energy production. One of the widely used MPPT algorithms is the Incremental Conductance (INC) algorithm. It is also superior to the Perturb and Observe (P&O) approach because it functions well even when there are rapid fluctuations in sunlight. However, MPPT alone is insufficient to drive motors [2] because these motors require a high and constant voltage that cannot be supplied by solar panels. Induction motors are used in farming and industry because of their power, cost-effectiveness, and low maintenance. However, the use of solar power to power these motors is not straightforward owing to fluctuations in the voltage of the solar panels. A large step-up DC-DC converter and inverter are required to maintain the power at a constant level. This is particularly suitable for a positive-output super-lift Luo (POSLL) converter. It offers a high voltage, low ripple, and better efficiency than traditional converters. This is beneficial when employed together with the INC MPPT algorithm to obtain a larger amount of energy and maintain a constant voltage [3]. A Voltage Source Inverter (VSI) is also necessary to convert DC power into AC power for use in changing-speed motors [4]], [5].

Building on the foundational understanding of MPPT techniques, this review delves into a comparative analysis of major methods, emphasizing the advantages of the INC method under rapidly fluctuating irradiance conditions. This also implies that INC outperforms P&O because it reduces oscillations and converges faster [6]. The authors [7] presented a better INC algorithm that increases dynamic tracking during rapid changes in irradiance; they found it to be more accurate and to have a smaller steady-state error than the traditional INC approach. This author [8] discussed the POSLL converter, whose geometry enables it to deliver a voltage lift, and observed that POSLL converters have a better voltage gain than normal boost converters, making them suitable for PV applications. In this study, P&O and INC were compared with the combination of MPPT and a Super-Lift Luo converter [9]. It has been found that the INC combined with the Luo converter offers a more stable output and better tracking efficiency. This study [10] shows that the Super-Lift Luo converter breaks the PV output voltage by a very large margin compared with the ripple of the conventional boost topology and the conversion efficiency. The authors [11] developed a one-stage INC MPPT structure that reduced the complexity of the system and reported that they achieved improved tracking with the least number of oscillations around the maximum power point. In this review [12], different high-step-up converters are grouped, and their suitability for renewable systems is discussed, with special attention to the fact that Luo converters and Super-Lift converters have a higher gain without the use of transformers. The author [13] discussed independent PV-powered induction motors with either single-stage or two-stage converters, including the significance of the constant DC-link voltage and the effectiveness of MPPT in keeping the pace of the motor with a varying amount of sunlight.

Independent PV systems used to provide motor drive functions face significant performance problems owing to changes in solar irradiance and temperature, resulting in erratic output voltage and reduced power supply. PV modules do not work consistently at the Maximum Power Point, especially when the conditions change rapidly. Conventional MPPT techniques, such as Perturb and Observe, cannot track the maximum power in changing situations. In addition, to drive an induction motor, a stable and sufficiently large DC-link voltage is required, which cannot be provided directly by a standard PV output. Traditional DC-DC converters cannot achieve the high voltage gain and regulation required for reliable motor operation. This leads to reduced motor performance, poor efficiency, and system unreliability in standalone PV-driven applications.

To address the limitations mentioned above, this study presents a combined standalone photovoltaic motor drive system consisting of an Incremental Conductance (INC)-based MPPT algorithm, a positive-output super-lift Luo (POSLL) DC-DC converter, and a voltage source inverter controlled by space vector PWM (SVPWM). The INC algorithm enhances the accuracy of tracking rapid irradiance variations, whereas the POSLL converter offers a high voltage gain with a lower ripple, making the DC-link voltage constant. The use of SVPWM improves the voltage use and dynamic response of the motor drive, which leads to faster settling time and reduced torque oscillations compared with traditional SPWM. The proposed model enhances the stability and efficiency of the entire system in a standalone implementation, with the main goal of improving the MPPT accuracy, voltage boosting capacity, and inverter-level control. Although photovoltaic-driven motor systems have been extensively studied, there are still several limitations to the current methods. Traditional MPPT methods, such as Perturb and Observe (P&O), have steady-state oscillations and slow convergence under fast-varying irradiance conditions, resulting in power loss and erratic DC-link voltage. Numerous reported systems use traditional boost or SEPIC converters, which have only a small voltage gain, and the ripple and efficiency deteriorate with increasing duty cycles. Moreover, many studies have concentrated on either the performance of MPPT or the analysis of converters; however, they have not confirmed the co-effect on motor-drive dynamics. Moreover, inverter control techniques, such as sinusoidal PWM (SPWM), which are commonly used in standalone PV-fed motor drives, lead to longer settling times and larger torque ripples during startup, speed change, and load disturbances. These constraints make current systems less likely to be used in reliable off-grid motor-drive applications.

The novelty of this study is that it integrates and quantitatively validates a system-level INC-based MPPT-controlled positive-output super-lift Luo converter with SVPWM-based inverter control of a standalone photovoltaic-fed induction motor drive. This work is in contrast to the current literature, which explores the algorithms of MPPT, converters, and inverter control in isolation; in other words, it shows how all these phases of energy transformation work together. In addition, the comparative analysis of SPWM and SVPWM under the same photovoltaic and load conditions provides clear numerical support for the performance improvement in terms of settling time, torque smoothness, and efficiency in off-grid applications.

2 Proposed PV System Description

The arrangement of an independent photovoltaic (PV)-powered system used to power an AC motor load is shown in Figure 1. In this arrangement, the PV array is the energy source and produces a DC output that is dependent on the solar irradiance and cell temperature. To utilize solar energy to its optimum, a maximum power point tracking (MPPT) system continuously adjusts the operating point of the PV array and provides the required duty ratio reference to the Luo DC-DC converter. The PV voltage was raised to the required level using a Luo converter, which was selected owing to its capability to produce a high step-up voltage gain with increased efficiency[14]. A three-phase voltage source inverter (VSI) then converts the adjusted DC output into AC power based on various leading modulation techniques, such as Sinusoidal Pulse-Width Modulation (SPWM) and Space Vector Pulse-Width Modulation (SVPWM). The output filter suppresses the switching harmonics and produces a clean AC waveform. The AC power was then fed to the motor, and the target reference and closed-loop control system measured the actual motor speed against the target reference and dynamically adjusted the switching signals of the inverter to keep the drive system operating steadily and efficiently under different load and environmental conditions[15]. **[Figure 1]**

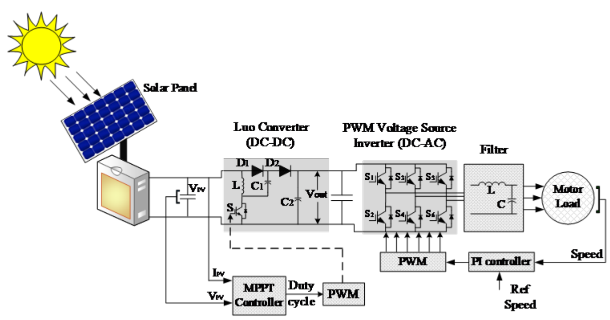

Fig 1. Block diagram representation of PV system with INC MPPT tracking.

The total efficiency of a standalone PV-driven system is determined by the combined efficiencies of the PV array, MPPT algorithm, and inverter. This is represented as[16],[17]

$$\eta_{Total} = \eta_{PV} \cdot \eta_{MPPT} \cdot \eta_{Inverter} \tag{1}$$

Alternatively, it can be formulated in terms of the power ratio as

$$\eta_{Total} = \frac{P_{OUT}}{G \bullet A} = \frac{P_{PV}}{G \bullet A} \bullet \frac{P_{MPPT}}{P_{PV}} \bullet \frac{P_{OUT}}{P_{MPPT}} \tag{2}$$

Where

η_{Total} Total efficiency of the PV-based conversion system

η_{MPPT} Efficiency of the MPPT tracking algorithm

$\eta_{Inverter}$ Efficiency of the inverter stage

η_{PV} Conversion efficiency of the PV module

$\boldsymbol{P}_{PV}$ Maximum power generated by the PV array

$\boldsymbol{P}_{MPPT}$ Power tracked by the MPPT controller

$\boldsymbol{P}_{OUT}$ Final AC output power delivered to the load

G Solar irradiance (W/m^2)

A Effective surface area of the PV array (m^2)

2.1 Maximum Power Point Tracking (MPPT)

Maximum Power Point Tracking (MPPT) is a crucial technology in photovoltaic (PV) systems that enables the system to adjust its power output as the environment changes. MPPT algorithms dynamically adjust the electrical operating point of PV modules to provide the maximum possible power to the system and enhance its efficiency[18],[19]. One widely used MPPT algorithm is the Incremental Conductance (INC) algorithm, which is based on the concept of measuring instantaneous conductance (I/V) against incremental conductance (dI/dV). This method works better than Perturb and Observe (P&O) when atmospheric conditions change[20],[21]. The INC algorithm responds quickly to irradiance variations, has minimal oscillation about the Maximum Power Point, and performs well under changing weather conditions. The application of MPPT typically requires DC-DC converters, such as the Luo converter, to boost the output voltage. The duty cycle of the PV panels matched the source impedance to the load impedance. As PV technology improves, MPPT algorithms increase the energy output and make solar power more economical[18].

2.1.1. Incremental Conductance algorithm

The incremental conductance (IC) algorithm is another advanced technique for maximum power point tracking (MPPT) used in photovoltaic systems to maximize the power output under different conditions. The performance of the IC algorithm is better than that of conventional techniques, particularly for rapidly changing irradiances[22]. The IC algorithm operates on the principle that the slope of the power-voltage curve is zero at the Maximum Power Point. It measures incremental and instantaneous conductance to determine the direction for adjusting the operating points. The IC algorithm can run at a steady state at the maximum power point and has fewer oscillations than the perturb and observe algorithm. The working mechanism of the IC algorithm is represented in the flowchart in Figure 2, which shows the decision-making process of the IC algorithm[22],[23]. The algorithm repeats its cycle as the operating point changes to maximize the power output under varying conditions. **[Figure 2]**

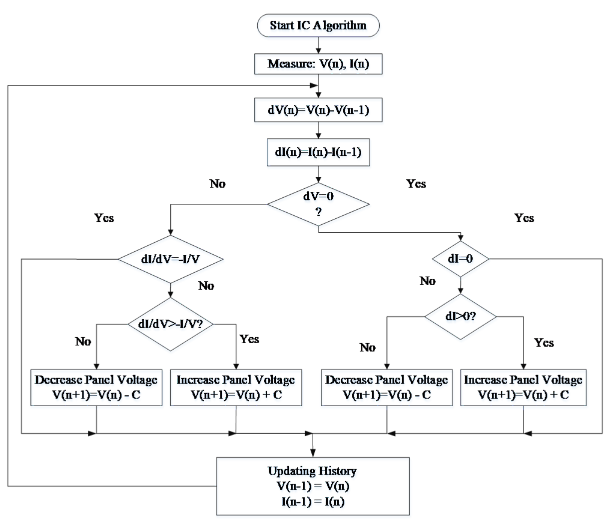

Fig 2. Flowchart of Incremental Conductance Algorithm

2.2 Solar Panel (DC Source)

The SunPower 305-WHT module utilized in the proposed system comprised 96 cells and offered a capacity of 300 W at 1000 W/m^2 and 25°C. Figure 3 illustrates the V-I and P-V characteristics of the proposed PV panel (SunPower SPR-305-WHT) under various temperature conditions. It can be observed that the panel's maximum power point is achieved at 300 W, 220 W, and 150 W with irradiance levels of 1000 W/m^2, 750 W/m^2, and 500 W/m^2, respectively, all at a temperature of 25°C[24]. The solar panel parameters are presented in Table 1. **[Figure 3] [Table 1]**

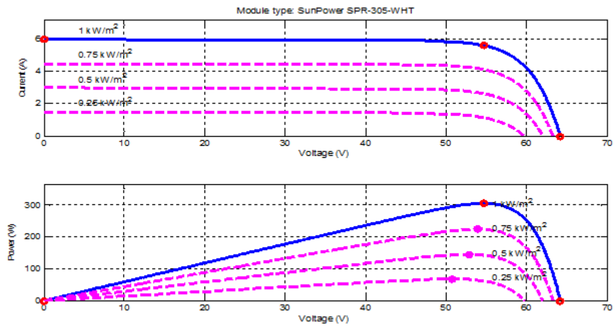

Fig 3. V-I and P-V characteristics for four irradiation levels of sun power SPR-305-WHT module.

Table 1. Electrical characteristics of the used PV module (SPR-305-WHT)

Parameters	Rating
Peak Power (+/- 5%) P_{max}	305 W
Rated Voltage V_{mpp}	54.7 V
Rated Current I_{mpp}	5.58 A
Open Circuit voltage V_{oc}	64.2 V
Short Circuit Current I_{sc}	5.96 A
Temperature coefficient of open – circuit voltage	-0.27 %/∘C
Temperature coefficient of short –circuit current	0.057 %/∘C

It is widely recognized that the temperature of PV panels (T) and the level of irradiation (I_{rr}) significantly influence the power output of PV systems. To enhance the efficiency of the system, an Incremental Conductance MPPT algorithm was employed to optimize the power extraction from the PV panel.

2.3 Luo converter (DC-DC Converter)

This configuration requires a positive-output super-lift Luo (PSLL) converter. Unlike traditional step-up converters, the PSLL Luo converter employs a dedicated voltage lift mechanism that increases the output voltage in discrete stages using a super-lift. This design innovation allows the converter to have a very high voltage gain and still have a lower current ripple, better efficiency, and better voltage regulation than the traditional boost and SEPIC converters. The working principle of the PSLL converter is the energy-transfer mechanism of inductors and capacitors, and the equivalent circuit of the PSLL converter can operate in two modes: switch-off and switch-on. The switch-on phase causes the inductors to store energy, and the switch-off phase causes the energy to be transferred to the load and capacitor, which amplifies the output voltage. The use of this staged voltage-lift principle makes the PSLL Luo converter particularly favorable for photovoltaic (PV) sensors, where a large voltage step-up is frequently required to synchronize with the inverter DC-link levels when used in standalone and grid-connected systems[25],[26]. **[Figure 4]**

Figure 4 shows the simplified structure of the PSLL Luo converter and the operation mode of the converter when the switch is in the conduction and cutoff states, respectively. These modes enable the interplay between the storage components of energy (inductors and capacitors) and the switching device to allow continuous passage of energy and a high voltage gain. Luo-based converter configurations in combination with MPPT and PI control have been highly cited in the recent literature as an effective remedy for high-performance solar PV systems[16],[17],[27]. The voltage across capacitor C1 is charged to V_{in}. During the switch-on period kT, the current i_L through inductor L increases with voltage V_{in}, and during the switch-off period (1-k) T, it decreases with voltage – (V_O - 2V_{in}). Consequently, the ripple in the inductor current iL is as;[27]

$$\Delta i_{L1} = \frac{V_{in}}{L} kT = \frac{V_o - 2V_{in}}{L}(1-k)T \tag{3}$$

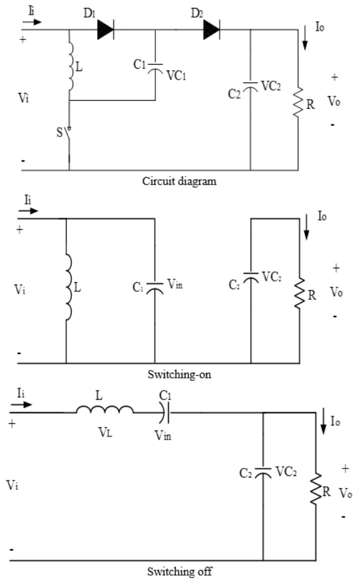

Fig 4. Positive output super-lift Luo (DC-DC) converter.

$$V_o = \frac{2-k}{1-k} V_{in} \tag{4}$$

The voltage transfer gain is as,

$$G = \frac{V_o}{V_{in}} = \frac{2-k}{1-k} \tag{5}$$

When the switch is on, the input current i_{in} is the sum of i_L and i_{C1}, whereas it is equal to i_L when the switch is off. During the switch-off phase, the current through capacitor i_{C1} matched that of i_L. In the steady state, the average charge on capacitor C1 must remain constant. The following equations are applicable:

$$i_{in-off} = i_{L-off} = i_{C1-off}$$

$$i_{in-on} = i_{L-on} = i_{C1-on}$$

$$kTi_{C1-on} = (1-k)Ti_{C1-off} \tag{6}$$

If inductance L is sufficiently large, i_L is nearly equal to its average current, I_L. So,

$$i_{in-off} = i_{C1-off} = I_L$$

$$i_{in-on} = I_L + \frac{1-k}{k} I_L = \frac{I_L}{k}$$

$$i_{C1-on} = \frac{1-k}{k} I_L \tag{7}$$

The average input current is.

$$i_{in} = ki_{in-on} + (1-k)i_{in-off} = I_L = (2-k)I_L \tag{8}$$

Considering,

$$\frac{V_{in}}{I_{in}} = \left(\frac{1-k}{2-k}\right)^2 \frac{V_o}{I_0} = \left(\frac{1-k}{2-k}\right)^2 R \tag{9}$$

The fluctuation of the current I_L through inductor L is,

$$\xi = \frac{\Delta i_L/2}{I_L} = \frac{k(2-k)TV_{in}}{2LI_{in}} = \frac{k(1-k)^2}{2(1-k)}\frac{R}{fL} \tag{10}$$

Normally, ξ is small, which means that this converter normally works in continuous mode.

The ripple voltage of output voltage v_o is

$$\Delta v_o = \frac{\Delta Q}{C_2} = \frac{I_o(1-k)T}{C_2} = \frac{1-k}{fC_2}\frac{V_o}{R} \tag{11}$$

The variation ratio of output voltage v_o is,

$$\varepsilon = \frac{\Delta v_o/2}{V_o} = \frac{1-k}{2RfC_2} \tag{12}$$

3 Results and Discussion

The proposed method was simulated using MATLAB/Simulink software, as shown in Figure 5. The SPR-305 PV panel was connected to the Luo converter to increase its working power. The irradiance of the PV panel was adjusted to the duty cycle of Luo by adjusting the incremental conductance MPPT controller, which adjusted the duty cycle. This was then fed to an inverter after passing through a Luo converter. The output of the pulse-width modulated inverter was linked to a three-phase induction motor. The speed of the motor was controlled by changing the inverter switches with PWM signals to a PI controller in accordance with the reference speed. [**Figure 5**]

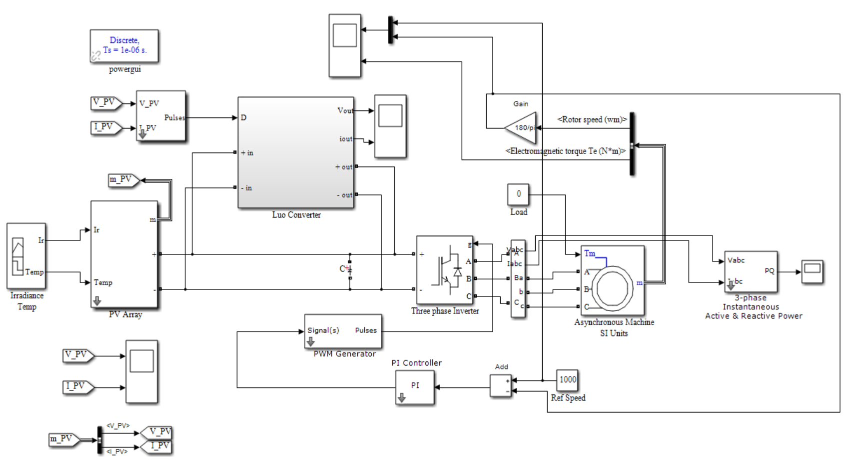

Fig 5. Simulink model of the proposed system.

The amount of solar irradiation and temperature variations are major considerations in determining the output of a PV system for any application. An Incremental Conductance algorithm was used to adjust the duty ratio to make the output of the Luo converter almost constant. The irradiance of the PV panel was decreased from 1000 to 200 W/m^2 in the period between t=0.7 and t=1.8s and the temperature remained constant at 25°C. In this phase, the power was reduced to 20 kW at 1.2s and then to 75 kW at 1.6 seconds. This was verified by the converter output voltage beating slightly 250V–280V at 1.2s owing to a variation in the duty ratio between 0.5 and 0.2, and the voltage was once more increased to 0.4 at 1.8s. As noted, the output of the proposed converter was almost constant (250V) even though there were changes in the irradiance and temperature under different climatic conditions. Figure 6 shows the modelling nature of the PV system under startup-transient conditions, with the inverter driven by SPWM. The results showed that although SPWM is a viable technique for generating balanced three-phase voltages, it leads to significant oscillations in the current output and electromagnetic torque, principally because of switching voltage ripples. Consequently, the motor converged gradually and reached a steady level after approximately 0.364s. At this point, the system achieved a steady-state torque of 4.127 N-m and an efficiency of 95.84%, highlighting the shortcomings of SPWM in terms of transient response and torque ripple. Figure 6 presents the respective responses for the SVPWM method. SVPWM revealed a much faster dynamic response, with the steady state of the motor speed attained at 0.1232s. The torque profile was also smoother and less oscillatory, and the steady-state efficiency was significantly increased, reaching 98.46%. The above results strongly indicate the better performance of SVPWM compared with SPWM when using standalone PV-fed motor-drive applications. The SVPWM approach not only provides faster convergence of speed and lower torque ripple but also provides better approximate overall performance and is therefore more amenable to high-performance renewable energy-based motor drives. [**Figure 6**]

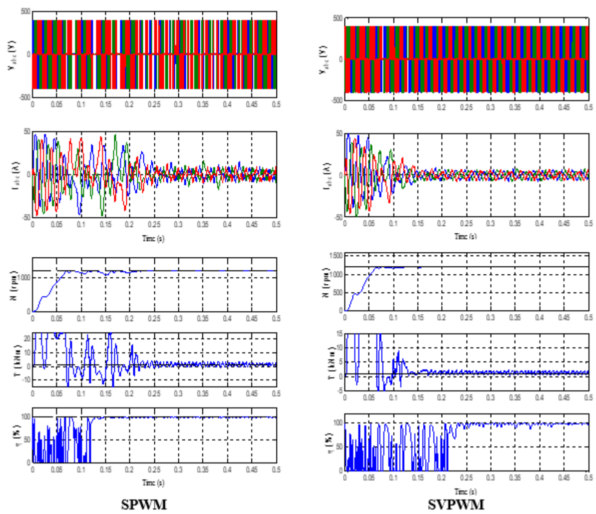

Fig 6. Startup-transient response of three-phase standalone PV system.

Figure 7 shows the response of the output voltage, current, speed, torque, and efficiency of a standalone photovoltaic (PV)-fed motor drive to a servo test with a 15% speed increase under the action of SPWM control. In this case, the reference speed at t = 0.5 seconds is decreased to 1400 rpm compared with 1200 rpm. It takes the motor 0.086s to reach the new steady-state speed at which it reaches a torque of 1.875 N-m and an efficiency of 98.64%. Figure 7 shows the corresponding response using SVPWM. The system in this case exhibited better dynamic performance, whereby the motor reached the commanded speed in 0.053 s. The torque response was smoother and restricted to 1 Nm, and the efficiency was enhanced to 99.47, which is a clear indication of the benefits of SVPWM in dynamic tracking. [**Figure 7**]

Figure 8 shows the response to a 30% slowdown in speed with the use of SPWM, whereby the speed of 1400 rpm reduces to 1000 rpm at t = 1.5 s. Under SPWM, the torque reached a steady point of 0.7 N-m, and the efficiency was 98.45%. In addition, Figure 8 shows a similar situation when controlled by SVPWM. In this case, the torque reduces slowly to zero, and the efficiency is 100% in the steady state. These results show that SVPWM has a shorter settling time, reduced torque ripples, and increased efficiency than traditional SPWM; consequently, it is a better choice than traditional SPWM in the servo control of independent PV-fed motor drive systems. [**Figure 8**]

Figure 9 shows the output voltage, current, speed, torque, and efficiency responses of the PV-powered motor drive under the conditions of regulation with sinusoidal PWM (SPWM) when the load torque is doubled. The applied torque is 10 N-m and then 15 N-m at t = 0.5s, which creates a significant disruption to the response of the motor. This short-term period also shows a slight reduction in speed and stabilization of the motor at 961.1 rpm, and the entire efficiency of the system reduces to 81.13% owing to the increased demand. In addition, it represents the corresponding response in the SVPWM. In this case, the system

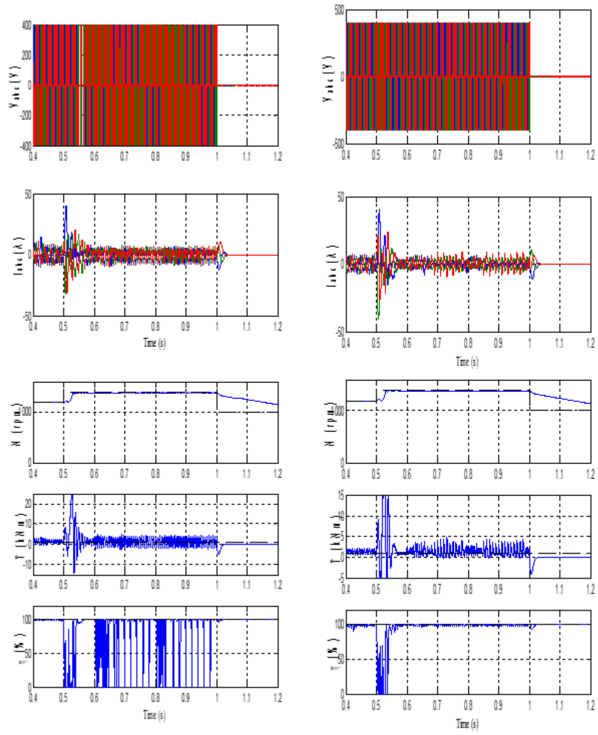

SPWM SVPWM

Fig 7. Servo responses of the proposed system with an increment of speed 15%.

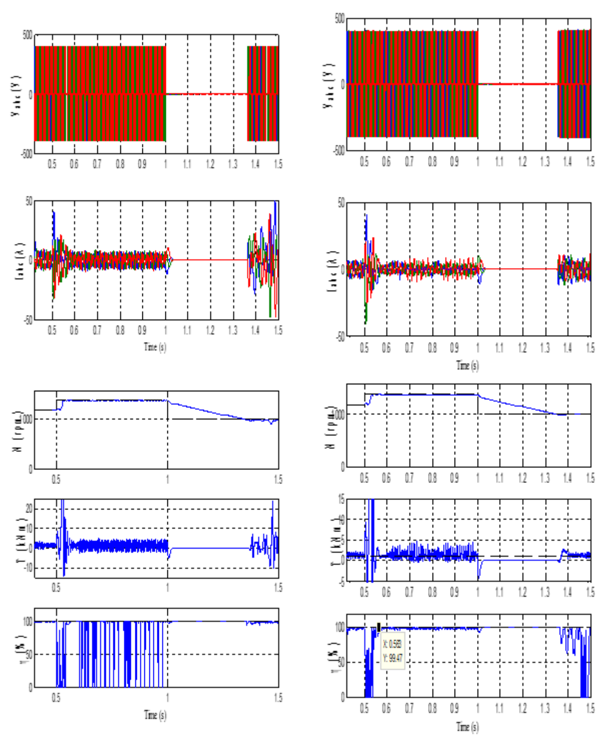

SPWM SVPWM

Fig 8. Servo responses of the proposed system with a decrement of speed 30%.

was more stable and had better dynamic performance. Although the torque also increased to 15 Nm, the efficiency decrease was not as significant as that of the SPWM. The efficiency of the system reached 87.55%, which indicates that SVPWM can be more efficient and perform better based on various load situations. [**Figure 9**]

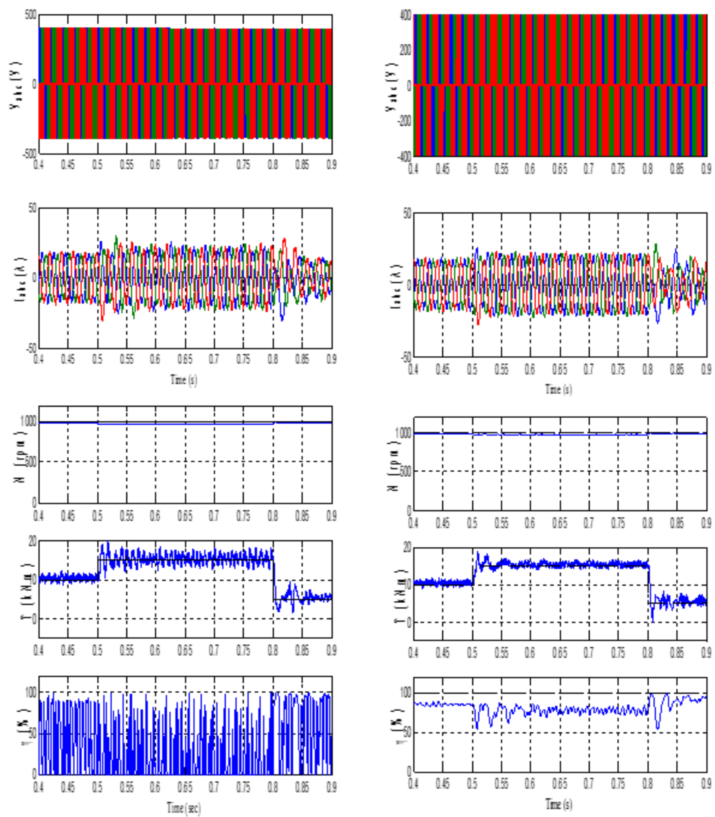

SPWM SVPWM

Fig 9. Regulatory response of the proposed system with load change of 50% increment.

Similarly, Figure 10 shows the output voltage, current, speed, torque, and efficiency of the standalone PV-driven motor drive during a regulatory test with a 75% load reduction under SPWM control. The motor torque decreased owing to the reduction in load, which caused the motor speed to increase. Under SPWM, the speed was 983 rpm, and the efficiency of the system was stabilized at 94.24%. This figure also displays the respective responses of SVPWM. In this case, the motor operated more efficiently, the speed increased to 996 rpm, and the system efficiency increased to 96.45%. The transition in torque was smoother and less oscillatory, and the efficiency profile of the system was more stable than that of the SPWM. The results of the study show that SVPWM has been found to have better dynamic control, higher efficiency, and better speed response under load-reduction operating conditions than standard SPWM, thereby proving its capability over conventional SPWM in regulating responses in PV-driven motors. [**Figure 10**] [**Table 2**] [**Table 3**]

Table 2. Simulated responses of PV Source Standalone System

Control Technique	**Start–up Transients**			**Servo response**				**Regulatory response**			
				Increment of 15%		**Decrement by 30%**		**Increment by 50%**		**Decrement by 75%**	
	Rise time (Sec)	**Settling time (Sec)**	**Efficiency (%)**	**Settling time (Sec)**	**Efficiency (%)**	**Settling time (Sec)**	**Efficiency (%)**	**Settling time (Sec)**	**Efficiency (%)**	**Settling time (Sec)**	**Efficiency (%)**
SPWM	0.5	0.364	95.84	0.086	98.64	0.285	98.45	0.137	81.13	0.158	94.24
SVPWM	0.0445	0.1232	98.46	0.053	99.47	0.168	100	0.0634	87.55	0.152	96.45

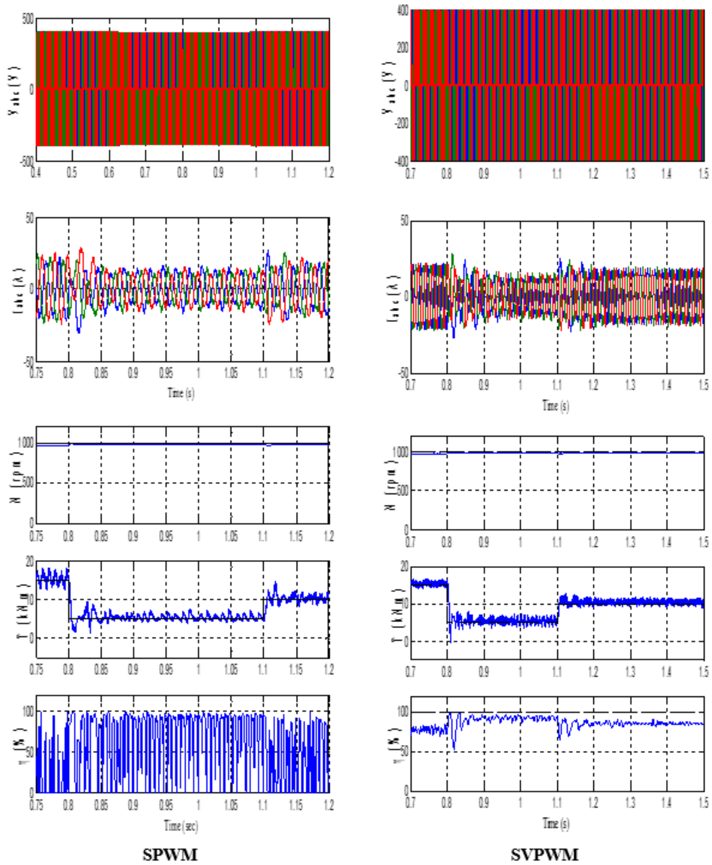

Fig 10. Regulatory response of the proposed system with load change of 75% decrement.

Table 2 shows the reactions of a standalone PV-fed motor drive system under various conditions. It compares two control schemes: SPWM and the SVPWM. Three conditions, namely the startup, servo, and regulatory responses, were used to measure the performance in terms of the rise time, settling time, and efficiency. SVPWM is superior for start-ups. The settling time of the SPWM was 0.364s, and it settled at 95.84%. The SVPWM stabilized after 0.1232s and had an efficiency of 98.46%. This implies that SVPWM is more responsive, consumes less energy, and the system is more stable and efficient. SVPWM is also superior in terms of the servo responses. At a 15% speed increase, the SPWM stabilized in 0.086s at 98.64% efficiency. With an efficiency of 99.47%, the SVPWM settled at 0.053 s. At a 30% reduction in speed, SPWM can take 0.285s with 98.45% efficiency, and SVPWM can take 0.168s with 100% efficiency. SVPWM is more responsive, allows change tracking, and minimizes changes in speed and torque. SVPWM is superior in terms of regulatory response. At 50% load, the SPWM stabilized at 0.137 s with an efficiency of 81.13%. The settling time of SVPWM was 0.0634 s, and it settled with an efficiency of 87.55%. With a load reduction of 75%, the SPWM required 0.158s with 94.24% efficiency, whereas the SVPWM required 0.152s with 96.45% efficiency. SVPWM is more responsive to loads and is more stable and efficient in terms of energy consumption than SPWM. Overall, Table 2 demonstrates that SVPWM is superior to SPWM under all conditions. This allows for quicker settling, minimizes variations in speed and torque, and is more efficient. In PV-based motor drives, performance and efficiency are important, and SVPWM is preferable.

Table 3 presents a comparative evaluation of the proposed standalone photovoltaic-fed induction motor drive with related studies reported in the literature. Prior studies primarily used conventional boost-type DC–DC converters and SPWM-based inverter controls often exhibit longer settling times and reduced efficiency under standalone operating conditions. The proposed system integrates an INC-based MPPT algorithm with a positive-output super-lift Luo converter and SVPWM-controlled inverter, resulting in improved voltage stability and dynamic response. As shown in Table X, the settling time is reduced by up to 66.15%, whereas the overall efficiency improves by approximately 2.6–6.4% compared with SPWM-based systems. Unlike several existing studies that validate individual subsystems independently, the results demonstrate a coordinated system-level improvement, confirming the suitability of the proposed approach for off-grid photovoltaic motor drive applications.

Table 3. Comparative Performance of the Proposed PV-fed Induction Motor drive with Existing Literature

Reference	MPPT Algorithm	DC–DC Converter	Modulation Technique	Application	Performance Metrics	Remarks
Saady *et al.*, (2021) [4]	P&O	Conventional DC–DC	SPWM	PV pumping system	Longer settling, torque oscillations	Limited transient performance
Bollipo *et al.*, (2020) [6]	INC	Boost	SPWM	Standalone PV	Settling time > 0.25 s, noticeable torque ripple	Moderate dynamic response; limited voltage gain
Shang et al., (2020) [7]	Improved INC	Boost	SPWM	PV system	Reduced MPPT oscillations, slow motor convergence	MPPT improved but inverter dynamics not optimized
Dheeban *et al.*, (2021) [10]	P&O / INC	Super-Lift Luo	—	PV source only	High voltage gain, ripple reduced	Converter validated without motor load
Oliver *et al.*, (2022) [14]	INC	Boost	SVPWM	Grid-interactive PV	Efficiency ≈ 95%	Grid support improves stability
Proposed System (Startup Transient)	**INC**	**POSLL Luo**	**SPWM**	**Standalone PV Motor Drive**	Settling time **0.364 s**, efficiency **95.84%**	Baseline comparison within proposed framework
Proposed System (Servo)	**INC**	**POSLL Luo**	**SVPWM**	**Standalone PV Motor Drive**	Settling time **0.1232 s**, efficiency **98.46%**	**66.15% faster response**, reduced torque ripple
Proposed System (Regulatory)	**INC**	**POSLL Luo**	**SVPWM**	**Standalone PV Motor Drive**	Efficiency **87.55% at 50% load, 96.45% at 75% load reduction**	Superior disturbance rejection

4 Conclusion

This study presents a standalone photovoltaic-fed induction motor drive system that combines an MPPT algorithm based on Incremental Conductance (INC), a positive-output super-lift Luo (POSLL) DC-DC converter, and a voltage source inverter that uses SPWM and SVPWM control methods. To test the system under dynamic conditions, the system's capabilities to respond to variable irradiance, speed, and load conditions were tested to determine the system's capabilities in terms of its overall efficiency and ability to regulate the voltage as required. The proposed configuration was proven to be effective through quantitative simulation studies. Even when the solar irradiance differed between 1000 W/m^2 and 200 W/m^2, the INC-based MPPT could maintain the power extraction constant and the DC-link voltage at approximately 250 V. The POSLL converter delivers the high voltage gain required with a lower ripple and allows the inverter to operate continuously and reliably under varying environmental conditions. The performance with SPWM was significantly worse than that with SVPWM. In the startup, the settling time decreased from 0.364s (SPWM) to 0.1232s (SVPWM), which is a 66.15% decrease. The steady-state efficiency was improved to 98.46% compared to 95.84%, and under load disturbance conditions, SVPWM had an efficiency of 87.55% compared to 81.13% at SPWM, indicating that it is more efficient in the disturbance rejection and response of the torque.

The novelty of this study is that it attempts to integrate and quantitatively compare an INC-MPPT-controlled POSLL converter with the SVPWM-based inverter control of a standalone photovoltaic-driven induction motor system. In addition, the direct numerical comparison between SPWM and SVPWM operating under the same photovoltaic and load conditions is another clear indication of the superiority of SVPWM in off-grid applications of renewable motors. Based on the obtained results, the proposed system can be successfully implemented in sun-powered irrigation pumps, rural industrial motor drives, and off-grid renewable energy needs, where a quick dynamic response and high efficiency are of high importance. To ensure practical implementation, SVPWM is highly recommended over SPWM because the former is more efficient with regard to settling time and operation during load disturbances. Future developments should be based on hardware realization, the addition of smart controllers (intelligent controllers, e.g., fuzzy or neuro-fuzzy controllers), and testing under partial shading and real-time operation conditions to make the system even more robust and applicable.

5 Acknowledgements

This research received no specific grant from any funding agency in the public, commercial, or not-for-profit sectors.

Conceptualization of study problem: Conceptualization of study problem: G Ashokkumar., Matlab/Simulink Design: G Ashokkumar., Data analysis: Dr. A Ravi., Research Guidance: Dr. R Kannan., Original Drafting; Editing & Reviewing: Dr. R Kannan.

References

1) Anowar MH, Roy P. Modified Incremental Conductance Based Photovoltaic MPPT Charge Controller. *Proceedings of the 5th International Conference on Electrical, Computer and Automation Engineering*. 2019. 10.1109/ecace.2019.8679308.
2) Khodair D, Shaker A, Motahhir S, Mostafa H, Abouelatta M, Munim H, et al. Modelling and Simulation of Modified MPPT Techniques under Varying Operating Climatic Conditions. *Energies*. 2023;16(1):549. 10.3390/en16010549.
3) Xu L, Wang Y, Solangi Y, Shah S, Zameer H. Off-Grid Solar PV Power Generation System in Sindh, Pakistan: A Techno-Economic Feasibility Analysis. *Processes*. 2019;7(5):308. 10.3390/pr7050308.
4) Saady I, Lamnadi M, Bossoufi B, Motahhir S, Majout B, Adouairi MS, et al. Optimization for a Photovoltaic Pumping System Using Indirect Field Oriented Control of Induction Motor. *Electronics*. 2021;10(24):3076. 10.3390/electronics10243076.
5) Maamar Y, Elzein IM, Benameur A, Mohamed H, Mahmoud MM, Mosaad MI, et al. A comparative analysis of recent MPPT algorithms (P&O/INC/FLC) for PV systems. *Journal of Robotics and Control (JRC)*. 2025;6(4):1581–1588. 10.18196/jrc.v6i4.25814.
6) Bollipo RB, Mikkili S, Bonthagorla PK. Critical review on PV MPPT techniques: Classical, intelligent, and hybrid approaches. *IET Renewable Power Generation*. 2020;14(9):1433–1452. 10.1049/iet-rpg.2019.1163.
7) Shang L, Wang Y, Hu Y. An improved MPPT control strategy based on incremental conductance. *Protection and Control of Modern Power Systems*. 2020;5(2):1–8. 10.1186/s41601-020-00161-z.
8) Shanmathi R, Karthikeyan A. A review on performance of positive output super-lift Luo converter. *AIP Conference Proceedings*. 2025;3021(1):020045. 10.1063/5.0286097.
9) Bharathi R, Kumar S. Super-lift Luo converter using MPPT strategy for photovoltaic systems. *AIP Conference Proceedings*. 2023;2865(1):040006. 10.1063/5.0155324.
10) Dheeban SS, Prabhu N, Elangovan D. Performance improvement of photovoltaic panels using Luo converter with super-lift technique. *International Journal of Power Electronics and Drive Systems*. 2021;12(3):1508–1517. 10.1016/j.matpr.2020.06.352.
11) Ali AIM, Abdelaziz AY, El-Naggar KM. An efficient MPPT technique-based single-stage incremental conductance approach. *Sustainability*. 2022;14(7):4026. 10.3390/su141912105.
12) Bai Y, Li J. High-efficiency high step-up DC–DC converters: A review. *Renewable and Sustainable Energy Reviews*. 2021;135:110191. 10.2478/v10175-011-0059-1.
13) Kumar K, Devi VL, Dhanamjayulu C, Kotb H, ELrashidi A. Evaluation and deployment of a unified MPPT controller for hybrid Luo converter in combined PV and wind energy systems. *Scientific Reports*. 2024;14:3248. 10.1038/s41598-024-53605-z.
14) Oliver JS, Mihet-Popa L, Balachandran PK, David PW. Analysis of Grid-Interactive PV-Fed BLDC Pump Using Optimized MPPT in DC–DC Converters. *Sustainability*. 2022;14(12):7205. 10.3390/su14127205.
15) Pavithra C, Sarathy RP, Palanivelrajan MP, Ladika S, Nagaraj PRK. Highly efficient maximum power point tracking control technique for PV system using different controller and converter with modular multilevel inverter. *EAI Endorsed Transactions on Energy Web*. 2024;11(1). 10.4108/ew.5216.
16) Asnil A, Refdinal N, Krismadinata K, Sonni MN. Performance Analysis of an Incremental Conductance MPPT Algorithm for Photovoltaic Systems under Rapid Irradiance Changes. *TEM Journal*. 2024;13(2):1087–1094.
17) Ghafour ZA, Ajel AR, Yasin NM. Super-Lift Luo Converter Using MPPT Strategy for PV System. *AIP Conference Proceedings*. 2023;2804(1):050012. 10.1063/5.0155324.
18) Ali MH, Zakaria M, El-Tawab S. A Comprehensive Study of Recent Maximum Power Point Tracking Techniques for Photovoltaic Systems. *Scientific Reports*. 2025;15(1):14269. 10.1038/s41598-025-96247-5.
19) Elsafi A, Almohammedi AA, Balfaqih M, Balfagih Z, Sabri S. Comparative analysis of maximum power point tracking methods for power optimization in grid tied photovoltaic solar systems. *Discover Applied Sciences*. 2025;7(9):976. 10.1007/s42452-025-07606-w.
20) Wajid A, Shah MQ, Nawaz F, Asif Q. Comparative Analysis of Maximum Power Point Tracking Algorithms for Solar Energy Systems. *IOSR Journal of Electronics and Communication Engineering*. 2025;20(3):19–35. 10.9790/2834-2003021935.
21) Ali MH, Zakaria M, El-Tawab S. A comprehensive study of recent maximum power point tracking techniques for photovoltaic systems. *Scientific Reports*. 2025;15(1):14269. 10.1038/s41598-025-96247-5.
22) Khaterchi H, Regaya CB, Jeridi A, Zaafouri A. Innovative hybrid war strategy optimization with incremental conductance for maximum power point tracking in partially shaded photovoltaic systems. *Power Electronics and Drives*. 2024;10(1):1–8. 10.2478/pead-2025-0001.
23) Bouarroudj N, Fezzani A, Benlahbib B, Batoun B, Drid S, Boukhetala D. Simulation and practical implementation under different scenarios of indirect incremental conductance algorithm for MPPT of PV system. *International Journal of Advanced Intelligence Paradigms*. 2025;30(2):131–151. 10.1504/IJAIP.2025.146973.
24) Ahmad EZ, Ibrahim A, Elbreki A, Fazlizan A, Jarimi H, Sopian K, et al. Recent advances in passive cooling methods for photovoltaic performance enhancement. *International Journal of Electrical and Computer Engineering (IJECE)*. 2021;11(1):146–154. 10.11591/ijece.v11i1.pp146-154.
25) Prasad DT, Anandhakumar R, Balamurugan P. Integration of Modified Luo Converter and ANFIS MPPT in Grid-Tied Photovoltaic Systems. *International Research Journal of Modernization in Engineering Technology and Science*. 2025. 10.54392/irjmt25322.
26) Dheeban SS, Selvan NBM, Krishnaveni L. Performance improvement of Photo-Voltaic panels by Super-Lift Luo converter in standalone application. *Materials Today: Proceedings*. 2021;37(2):1163–1171. 10.1016/j.matpr.2020.06.352.
27) Ananth SV, Singaravelu S. Modelling and Simulation of MPPT Based Solar Photovoltaic System for Voltage Lift Luo Converter. *International Journal of Electrical and Electronics Research*. 2023;11(1):90–96. 10.37391/ijeer.110112.